Carbohydrate Polymers 77 (2009) 394–401

Contents lists available at ScienceDirect

Carbohydrate Polymers

journal homepage: www.elsevier.com/locate/carbpol

Chitosan bearing pendant cyclodextrin as a carrier for controlled protein release

Xinge Zhang [a,*], Zhongming Wu [b], Xiujun Gao [a], Shujun Shu [a], Huijie Zhang [a], Zhen Wang [a], Chaoxing Li [a,*]

[a] Key Laboratory of Functional Polymer Materials of Ministry Education, and Institute of Polymer Chemistry, Nankai University, 94 Weijin Road, Tianjin 300071, China
[b] Metabolic Diseases Hospital, Tianjin Medical University, Tianjin 300070, China

ARTICLE INFO

Article history:
Received 20 November 2008
Received in revised form 29 December 2008
Accepted 15 January 2009
Available online 30 January 2009

Keywords:
Chitosan
β-Cyclodextrin
Nanocomplex
Drug delivery
Insulin

ABSTRACT

The objective of this work was to investigate the possibility of chitosan bearing β-cyclodextrin (CDen-*g*-CS) nanocomplexes for controlled protein release. CDen-*g*-CS was synthesized by a one-step procedure with *N*-succinylated chitosan and mono(6-(2-aminoethyl)amino-6-deoxy)-β-cyclodextrin in the presence of the water-soluble carbodiimide. The amount of β-CD grafted was up to 62.1 wt%. In vitro cytotoxicity against NIH 3T3 cells showed that CDen-*g*-CS was not cytotoxic and no significant difference of cytotoxicity was found between CDen-*g*-CS groups. Self-assembled nanocomplexes between CDen-*g*-CS and insulin were in the size range of 190–328 nm, with positive electrical charge (+3.7 to +25.5 mV) and high loading efficiency (37.7%). Insulin release in vitro was affected by the medium pH and the composition of copolymer. These results demonstrated that CDen-*g*-CS copolymer was a new promising vehicle for controlled protein release.

1. Introduction

Macromolecular aggregation, such as proteins and peptides, happens mainly by the interaction of hydrophobic residues in the molecules and is often accompanied by drastic reduction of biological potency in formulating drug delivery systems. Cyclodextrin (CD) complexation represents an effective strategy for improving macromolecular drug therapy by stabilizing them against aggregation, thermal denaturation and degradation. Macromolecular drugs can be partially complexed by CDs via their hydrophobic side chains (Irie & Uekama, 1999), and CDs' ability to sequester hydrophobic moieties helps in improving the stability of drugs. If only partially included into the CD cavity, the stability of the drugs can significantly be improved (Dotsikas & Loukas, 2002). Hydrophilic β-CD inhibits the adsorption of insulin to hydrophobic surfaces and prevents the self-aggregation of insulin at neutral pH (Lovatt, Cooper, & Camilleri, 1996), and the possible complexation sites for insulin monomers were characterized by Aachmann et al. and Lovatt et al. (Aachmann, Otzen, Larsen, & Wimmer, 1999; Lovatt et al., 1996). Additionally, CDs are known to enhance solubility of the incorporated drug (Filipović-Grčić et al., 2000), to act as permeation enhancers for macromolecular drugs (Merkus, Verhoef, Romeijn, & Schipper, 1991; Sakr, 1996; Yang et al., 2004) and to inhibit the activity of certain proteases (Matsubara, Ando, Iri, & Uekama, 1997). However, the clinical exploitation of CD has been restricted mainly due to perturbing the membrane fluidity to lower the barrier function. Moreover, since CDs are poorly adsorbed from the gastrointestinal (GI) tract following oral administration, the oral administration of CDs raises minimal safety concerns that may result from the systemic absorption of the CDs themselves. However, CDs may cause secondary systemic effects through increased GI elimination of certain nutrients and bile acids.

Recently, nanoparticulate systems have been identified as suitable peptide/protein carriers, which are able to protect the drugs from degradation, to improve permeation/penetration of the drugs across mucosal surface and also to control the release of the encapsulated drugs. CD complexed insulin encapsulated mucoadhesive nanoparticles seems to be a promising system for improving oral insulin delivery (Moses, Dileep, & Sharma, 2000; Victor & Sharma, 2002). Sajeesh and Sharma also demonstrated insulin absorption from GI tract by radioimmunoassay following an oral administration of CD-insulin complex encapsulated polymethacrylic acid matrix (Sajeesh & Sharma, 2006).

It is well known that chitosan (CS) is a natural polysaccharide which has been widely used in pharmaceutical areas thanks to its attractive biocompatibility, biodegradability, particle-forming property and antimicrobial activity (Ravi & Majeti, 2000; Vilivalam & Dodane, 1998). Both nasal and oral drug delivery research has demonstrated that significantly higher amounts of macromolecular drugs can be transported after co-administration with CS (Illum, Farraj, & Davis, 1994; Tozaki et al., 1997; van der Lubben, Verhoef, Borchard, & Junginger, 2001).

CD has the merit of a hydrophobic cavity which is easy to assemble with other molecule and CS can be slowly degraded in organism. Therefore, grafting CD molecules onto CS-reactive sites may lead to a molecular carrier that possesses the cumulative ef-

* Corresponding authors. Tel.: +86 22 23501645; fax: +86 22 23505598 (C. Li).
E-mail addresses: zhangxinge@nankai.edu.cn (X. Zhang), lcx@nankai.edu.cn (C. Li).

0144-8617/$ - see front matter Crown Copyright © 2009 Published by Elsevier Ltd. All rights reserved.
doi:10.1016/j.carbpol.2009.01.018

fects of inclusion, size specificity and transport properties of CD and mucoadhesive properties of CS (Prabaharan & Mano, 2006; Venter, Kotźe, Auźely-Velty, & Rinaudo, 2006). Different types of CD-grafted CS derivatives were designed as adsorbent matrices for the association and delivery of aromatic and other small organic molecules (Aoki, Nishikawa, & Hattori, 2003; Chen & Wang, 2001; Gaffar, El-Rafie, & El-Tahlawy, 2004; Prabaharan & Mano, 2005, 2006) and as antimicrobial agents (El-Tahlawy, Gaffar, & El-Rafie, 2006). Moreover, CS–CD delivery system has the mucoadhesive properties which can prolong the residence time for macromolecular drugs at the site of absorption (Venter et al., 2006).

Given these premises, the aim of the present work was to develop nanoparticulate systems based on the coupling of a mono(6-(2-aminoethyl)amino-6-deoxy)-β-cyclodextrin derivative with chitosan, intending for the delivery system of hydrophilic macromolecules, such as peptides and proteins. The preliminary cell viability of the materials was also evaluated. And the physicochemical properties of insulin/CDen-*g*-CS nanocomplexes were characterized and insulin release in vitro was further investigated.

2. Experimental

2.1. Materials

CS (degree of deacetylation 90%; with molecular mass of 6 and 20 kDa) was obtained from the Zhejiang Yuhuan Ocean Biochemical Co., Ltd. (Zhejiang, China). β-CD (purchased from the Sinopharm Chemical Reagent Co., Ltd., China) was recrystallized from water when used for binding experiments and used as received for preparation of monotosylate. Pure crystalline porcine insulin (with a nominal activity of 28 IU/mg) that was used without further purification was obtained from the Xuzhou Wanbang Biochemical Co., Ltd. (Jiangsu, China). 1-Ethy-3-(3-dimethylaminopropyl-carbodiimide) hydrochloride (EDC·HCl), and 1-hydroxybenzotrizole (HOBt) were purchased from the J&K China Chemical Ltd. (Beijing, China). All other chemicals were of analytical grade and purchased from local commercial sources.

2.2. Instruments and characterization methods

^{1}H NMR spectrum was recorded at room temperature on a Varian INOVA 500NB spectrometer at 400 MHz with tetramethylsilane as an internal standard and D_2O as solvent. Fourier transform infrared (FT-IR) analysis was performed on a Bio-Rad FTS 135 FT-IR spectrometer. The samples were mixed and ground with spectroscopic potassium bromide prior to being placed in the sample cell. All the diffuse reflectance spectra were scanned over the range 400–4000 cm^{-1}. Wide-angle X-ray diffraction measurement was performed on the powder and film samples using Rigaku D/max-2500 X type X-ray diffractometer (Ni-filtered, Cu Kα radiation with a wavelength of 0.154 nm). CD spectra were recorded on a Jasco-715 Spectropolarimeter (JASCO, Tokyo, Japan) at 25 °C under a constant flow of nitrogen gas. Typically a cell with a 0.1 cm path length was used for spectra recorded between 190 and 260 nm with sampling points every 0.1 nm. The spectra represent the average of 8–20 scans. CD intensities in the figures are expressed in (mdeg). The morphological examination of nanocomplexes was performed by transmission electron microscopy (Philips EM400ST). Samples were placed on copper grids with Formvar films for viewing under the microscope. Particle size and zeta potential were determined by photo-correlation spectroscopy (PCS, BI-200SM) and laser Doppler anemometry (Zetasizer 3000 HS), respectively. For the determination of the electrophoretic mobility, the samples were placed in electrophoretic cells where a potential of ±150 mV was established. The zeta potential was the average value of analysis in triplicate.

2.3. Synthesis of β-cycodextrin-grafted chitosan

2.3.1. Preparation of Mono-6-deoxy-6-(p-tolylsulfonyl)-β-cyclodextrin

Mono-6-deoxy-6-(p-tolylsulfonyl)-β-cyclodextrin (6-OTs-β-CD) was synthesized as described by the previously reported method (Petter et al., 1990). β-CD (20.0 g, 16.3 mmol) was suspended in 150 mL of water, and NaOH (2.16 g, 54.7 mmol) in 7 mL of water was added dropwise over 6 min. The suspension became homogeneous and slightly yellow before the addition was complete. *P*-toluenesulfonyl chloride (3.36 g, 17.6 mmol) in 10 mL of acetonitrile was added dropwise over 8 min, causing immediate formation of a white precipitate. After 2 h of stirring at 23 °C, the precipitate was removed by filtration and the filtrate was refrigerated overnight at 4 °C. The resulting white precipitate was recovered by filtration and after drying for 12 h it afforded 2.39 g of pure white solid in 11% yield.

2.3.2. Preparation of mono(6-(2-aminoethyl)amino-6-deoxy)-b-cyclodextrin

Mono(6-(2-aminoethyl)amino-6-deoxy)-β-cyclodextrin (CDen) was prepared via the reaction of 6-OTs-β-CD with freshly distilled ethyldiamine (Liu et al., 2003). Briefly, ethylenediamine (0.8 g) and 6-OTs-β-CD (4.0 g) were dissolved in water (30 mL) containing triethylamine (20 mL), and the stirred mixture was heated to reflux under nitrogen atmosphere for 24 h. After evaporation under reduced pressure, the residue was poured into the vigorously stirred anhydrous ethanol (500 mL), and the resultant mixture was stored in a refrigerator to produce a slight yellow precipitate. The crude solid product was collected by filtration and then purified by column chromatography on a hydroxymethylcellulose column with an aqueous ammonium bicarbonate eluent (0.05 mol/L), followed by chromatography on a Sephadex G-25 column with deionized water as eluent, to give white product (2.2 g) in 50% yield.

2.3.3. Preparation of N-(carboxyacyl) chitosan

N-(carboxyacyl) chitosan was prepared as described by Hirano and Moriyasu (Hirano & Moriyasu, 1981). CS (1.0 g) was dissolved in 100 mL of methanol containing 5% acetic acid (4/1, v/v). A solution of succinic anhydride (1.0 g) dissolved in acetone was added to CS solution with stirring at room temperature for 16 h. The reactive mixture was diluted with 100 mL of water, and pH was adjusted to 10 using 2 M NaOH. The reactant was dialyzed against distilled water for 5 days before the solution was freeze-dried. The substitute degree of succinic anhydride was 50 wt% by the element analysis.

2.3.4. Preparation of cyclodextrin-grafted chitosan (CDen-g-CS)

The typical coupling reaction procedure was as follows. *N*-(carboxyacyl) chitosan (85 mg, 0.40 mmol) and CDen (589 mg, 0.50 mmol) were dissolved in water/*N*,*N*-dimethylforamide (DMF) mixture with stirring at 0 °C for 1 h. EDC (959 mg, 0.50 mmol) and HOBt (676 mg, 0.050 mmol) were added to the above solution and stirred at 0 °C for 4 h, then at room temperature for 48 h. The pH was adjusted to 2 by the addition of 1 M HCl, and then dialyzed against distilled water for 5 days before the solution was freeze-dried.

2.4. Measurement of the apparent amount of grafting

Preparation of standard curve was conducted according to the procedure outlined previously (Dubois et al., 1956). The measurement was conducted as follows: β-CD-grafted CS (25 mg) was hydrolyzed in 15 mL of sulfuric acid (0.5 mol/L) and stirred for 10 h at 100 °C. The hydrolysate was gradually transferred to a measuring flask and diluted to 50 mL. The concentration of glucosyl

unit was determined with a spectrometer at 490 nm and transformed to the apparent amount of grafting. The apparent amount of grafting (Q) was calculated as follows:

$$Q = \frac{c \times 50 \times 1000}{180 \times 7 \times W} \quad (1)$$

where C is the concentration of glucose (μg/mL), and W is the weight of CDen-*g*-CS (mg).

2.5. Cell viability assay

Cell viability was evaluated by using NIH 3T3 cells. The cell line was cultured in Dulbecco's modified Eagle's medium (DMEM) (pH 7.4) in a humidified atmosphere (5% CO_2/95% O_2). The cells were seeded into 96-well plates with 10,000 cells per well. The plates were then returned to the incubator and the cells were allowed to grow to confluence for 24 h. CS and CDen-*g*-CS material dispersions were prepared with culture medium. The dispersions were diluted to give a range of final concentration from 5 to 100 mg/mL. Then the media in the wells were replaced with the pre-prepared culture medium–sample mixture (200 μL). The plates were then returned to the incubator and maintained in 5% CO_2 at 37 °C for 48 and 96 h, respectively. Each sample was tested in six replicates per plate. After incubation culture medium and 20 μL of thiazolyl blue tetrazolium bromide (MTT) solution was used to replace the mixture in each well. The plates were then returned to the incubator and incubated for further 4 h in 5% CO_2 at 37 °C. Then, the culture medium and MTT were removed. Isopropanol (100 μL) was then added to each well to dissolve the formazane crystals. The plate was placed in 5% CO_2 at 37 °C for 10 min and at 6 °C for 15 min before measurement. The optical density was read on a microplate reader at 570 nm. Cell viability was determined as a percentage of the positive control (untreated cells).

2.6. The preparation of insulin/CDen-g-CS nanocomplexes

The preparation of insulin/CDen-*g*-CS nanocomplexes was based on electrostatic interaction. Experiments were done to identify the production zone for formation of nanocomplexes. For this purpose, CDen-*g*-CS was dissolved in acetic acid (1%, w/v) at various concentrations of CDen-*g*-CS (0.5, 1.0, 1.5 and 2.0 mg/mL). Various concentrations of insulin solution (1.0, 2.0 and 3.0 mg/mL) were added dropwise to 5 mL of CDen-*g*-CS solution with stirring at room temperature. The samples were visually analyzed and three different systems were identified: clear solution, opalescent suspension (nanocomplexes) and aggregates. Preliminary study on the formation of nanocomplexes showed the concentration of CDen-*g*-CS was 2 mg/mL.

2.7. Evaluation of the insulin-loading capacity of nanocomplexes

The association efficiency of insulin was determined upon separation of nanocomplexes from the aqueous medium containing free insulin by centrifugation (16,000 rpm, 30 min, 15 °C). The amount of free insulin in the supernatant was measured by the Bradford method using a UV spectrometer (Shimadzu UV-2550) at 595 nm. The insulin loading capacity (LC) and the association efficiency (AE) were calculated as follows:

$$\mathrm{AE}\% = \frac{\text{total insulin} - \text{free insulin}}{\text{total insulin}} \times 100\%$$

$$\mathrm{LC}\% = \frac{\text{total insulin} - \text{free insulin}}{\text{nanocomplexes weight}} \times 100\%$$

All measurements were performed in triplicate and averaged.

2.8. In vitro release studies

Sample (2 mL) of the nanocomplexes was put in the dialysis membrane and then sealed at both ends with medicell clips. This then was immersed in 5 mL release medium, maintained at 37 °C in a water bath and dialyzed. At different time-intervals, 1 mL sample of the dialysis medium was taken. The amount of free insulin was determined by the Bradford method. In each experiment, the samples were analyzed in triplicate and the error bars in the plot were the standard deviation.

2.9. Analysis of release data

To determine the drug release mechanism and to compare the release profiles among nanocomplexes, the drug released amount versus time was used. We analyzed the release data with the following mathematical models:

$$M_t/M_\infty = k_1 t^n \text{ or } \log(M_t/M_\infty) = \log k_1 + n\log t \quad (2)$$

where M_t/M_∞ is the fractional amount of the drug released at time t, n is a diffusion exponent which indicates the release mechanism, and k_1 is a characteristic constant of the system. From the slope and intercept of the plot of log (M_t/M_∞) versus log t, kinetic parameters n and k_1 were calculated (Peppas, 1985). For comparison purposes, the data was also subjected to Eq. (3), which may be considered a simple, Higuchi equation.

$$M_t/M_\infty = k_2 t^{0.5}. \quad (3)$$

Eq. (3), for release data dependent on the square root of time, would give a straight line release profile, with k_2 presented as a root time dissolution rate constant.

3. Results and discussion

3.1. The synthesis of materials

The two components, containing a free carboxyl group and a free amino group, respectively, coupled in high yield upon treatment with EDC at room temperature. The existence of a hydroxyl group slightly affects this coupling reaction. Therefore, with the selective amino-bridged reaction of β-CDs, the coupling reaction of –COOH in *N*-(carboxyacyl) chitosan and $-NH_2$ instead of –OH of β-CDs can take place. The ^{1}H NMR spectrum of CDen-*g*-CS demonstrates that the peaks at δ 3.64 ppm were assigned to the protons on C^2–C^6 of CD and chitosan unit, which was due to that they had a similar six cyclic structure. Peaks at δ 5.0 ppm were assigned to C^1 methine protons signal on CD. Peaks at δ 2.6 ppm were methylene protons of succic acid on CS backbone, and peaks at δ 2.0 ppm were assigned to the protons of CH_3 on non-deacylated CONH content. FT-IR spectra of CDen-*g*-CS and CS show that the peak at 2930 cm^{-1} was $-CH_2$ vibrate bond and was increased, which was due to that $-CH_2$ groups were introduced by the reaction of succinic anhydride and CS. The peak at 1560 cm^{-1} was assigned to N–H vibrate bond and it disappeared if $-NH_2$ group of CS was completely substituted (Holme & Hall, 1992; Qu, Wirsen, & Albertsson, 2000; Kurita, 2001). From IR spectroscopy of CDen-*g*-CS, we know that the peak at 1560 cm^{-1} was weaken, which indicates that part of $-NH_2$ groups were substituted. Moreover, the sign at 892 cm^{-1} was the characteristic peak of β-(1,4) indican bond in CS, and its intensity was changed, which indicates that six cyclic structure of CS was destroyed. The peak at 843 cm^{-1} was attributed to C–H bending vibration of α-(1,4) glucopyranoside in β-CD. This shows that β-CD was grafted onto CS backbone.

The graft amount of CDen was not significantly affected by the molecular mass of CS. Moreover, graft amount was also invariable with an increase in the amount of β-CDen if the reaction was pro-

cessed in the water media, which was due to the poor solubility of CDen. However, the amount of β-CDen grafted increased by the addition of appropriate amount of DMF to the water media. From the results in Fig. 1, it can be seen that the amount of β-CDen grafted increased with an increase in DMF content. The amount of β-CDen in CDen62-*g*-CS20 was up to 62.1 μmol/g while the percentage of DMF was 20% (DMF/water, v/v); The amount of β-CDen in CDen60-*g*-CS6 was up to 60.3 μmol/g while the percentage of DMF was 30%. However, the percentage of DMF was further increased, the amount of β-CDen grafted decreased. This is due to the fact that the solubility of CDen increased by the addition of DMF and the excess DMF decreased the solubility of CS.

3.2. X-ray diffraction analysis

So far, at least seven polymorphs have been proposed for CS (Ogawa, Hirano, Miyanishi, Yui, & Watanabe, 1984; Saito, Ryoko, & Ogawa, 1987; Samuels, 1981), including "tendon-CS", "annealed", "I-2", "L-2", "form I", "form II", and "noncrystalline". Ogawa et al. have proposed three forms: noncrystalline, hydrated ("tendon") crystalline, and anhydrous ("annealed") crystalline (Pocker & Biswas, 1980). The hydrated crystalline structure gives a reflection at $2\theta = 10°$ (or peaks at around 8° and 12°), and the anhydrous crystalline structure gives one at $2\theta = 15°$. Fig. 2 illustrates the XRD patterns of neat CS and CS with the grafting β-CDen. CS shows characteristic peaks around $2\theta = 12.6°$, 19°, and 26°. The former peak corresponded to the hydrated crystalline structure, while the broaden peak around $2\theta = 21°$ indicated the existence of an amorphous structure. The results showed that incorporation of β-CDen affected the crystalline structure of CS, as supported by the XRD pattern of CDen-*g*-CS.

3.3. Cell toxicity assays

CDs are considered "high performance pharmaceutical excipients" (Irie & Uekama, 1997). Their toxicity has been evaluated, depending on the route of administration, the cavity size (α, β or γ-CD), and chemical modification (hydroxypropyl-CD, sulfobutylether-CD, CD sulphate and methylated CD). Therefore, it was important in the present project to verify the innocuous nature of the polymerized CD present on the surface of CS. We performed a series of experiments to evaluate CDen-*g*-CS potential toxicity. Fig. 3 shows the results of in vitro cytotoxicity of CDen-*g*-CS analyzed by the MTT method in NIH 3T3 cell line. As shown in Fig. 3A, various CDen-*g*-CS showed less cytotoxicity than that of CS within 48 and 96 h. We also conducted a dose response by exposing NIH 3T3 cells to various concentrations of CDen60-*g*-CS6 for 48 and 96 h (Fig. 3B). No toxicity

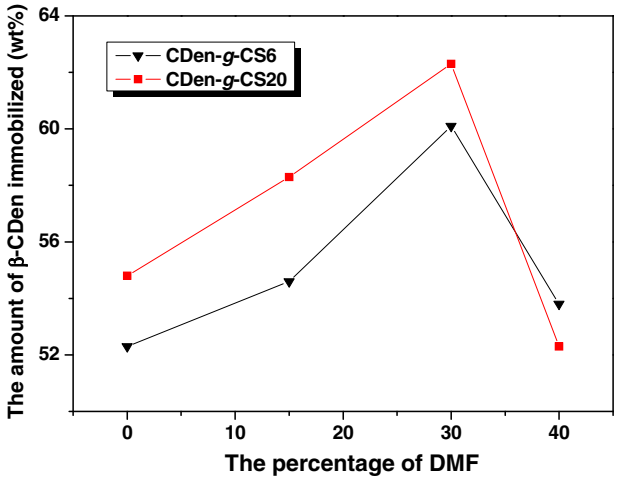

Fig. 1. Changes of the amount of β-CDen immobilized CS as the percentage of DMF.

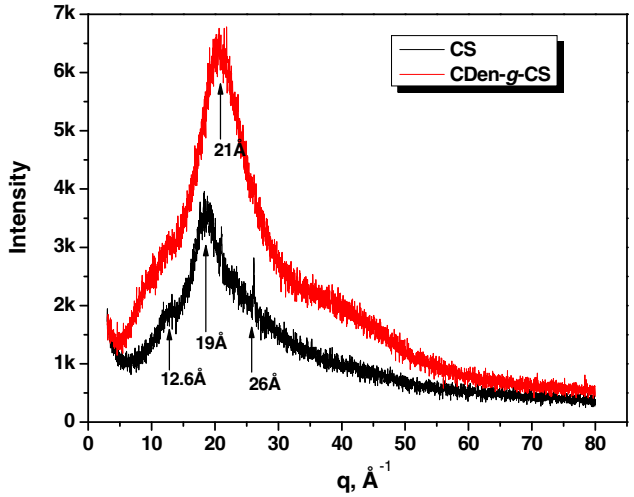

Fig. 2. X-ray diffraction spectra of CS and CDen-*g*-CS.

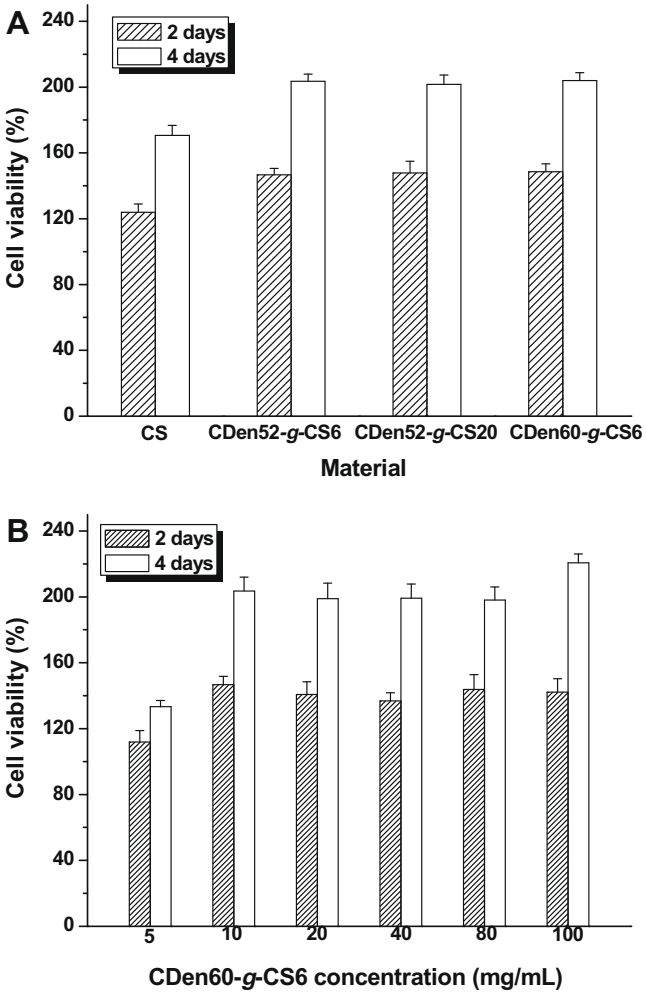

Fig. 3. Cell viability assay in NIH 3T3 cell line. The cells were treated with various materials (10 mg/mL of CS, CDen52-*g*-CS6, CDen52-*g*-CS20 and CDen60-*g*-CS6) (A) and various concentrations of CDen60-*g*-CS6 (5, 10, 20, 40, 80 and 100 mg/mL) (B) at 37 °C for 48 and 96 h, respectively. Cell viability was determined by the MTT assay and expressed as a percentage of control, that is, the untreated cell cultures.

(>111.93 ± 6.9%) was showed with an increase in the concentration of CDen60-*g*-CS6 (from 5 to 100 mg/mL) for 48 h. Time course experiments confirmed a significant increase of cell viability from 48 to 96 h (Fig. 3). The external component of CD, which contains many

hydrophilic hydroxide groups, could improve the interaction between CS and the cells. It may be attributed to the reduction of the density of amino groups by the introduction of β-CD in CDen-*g*-CS. Yang et al. reported that the introduction of α-CD decreased the cytotoxicity of polyether-imide (PEI). It is thought that the high amino density and high molecular weight were the reasons of the high cytotoxicity of PEI (Yang, Li, Goh, & Li, 2007).

3.4. Circular dichroism spectra

Fig. 4 exhibits spectra characteristic of the α-helix structure with two negative peaks around 223 and 208 nm in the CD spectrum of insulin. The helix content was estimated to be 25.98% from the value of the molar ellipticity at 223 nm in the insulin standard. The addition of CDen-*g*-CS affected the circular dichroism band indicated that the helix content of insulin (17.68%) was influenced by the addition of CDen-*g*-CS, suggesting that the intermolecular association between this peptide and CDen-*g*-CS decreased the content of insulin measured. Pocker and Biswas reported that the helix content depended on the concentration of insulin (Pocker & Biswas, 1980). This is because that the formation of insulin/CDen-*g*-CS complexes decreased the insulin content in solution. Thus, experimental evidence provides for the fact that insulin's tertiary structure has not been distorted.

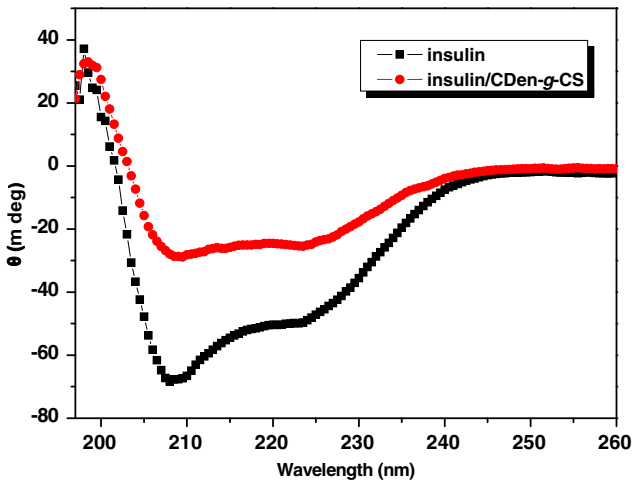

Fig. 4. The CD spectra of aqueous solution of (a) insulin alone, and (b) insulin/CDen-*g*-CS.

3.5. Characterization of insulin/CDen-g-CS nanocomplexes

The properties of the self-assembled insulin/CDen-g-CS nanocomplexes are summarized in Table 1. Nanocomplexes presented a sphere shape (Fig. 5) and had a size in the range of 190–330 nm with good dispersity (Table 1). For insulin/CDen62-*g*-CS20 nanocomplexes, increasing the concentration of insulin caused the mean particle size to increase with the same amount of β-CDen immoblilizated (62.1 μmol/g). However, Table 1 shows the particle size of insulin/CDen62-*g*-CS20 nanocomplexes was smaller than that of insulin/CDen60-*g*-CS6 with the same of insulin concentration. It is well known that shorter polymer chains give rise to smaller nanoparticles and the increase in mean size of the particles with increasing polymeric molecular mass is expected. However, nanocomplexes with the short-chain CS, CDen60-*g*-CS6, were unexpectedly larger than those produced from the long-chain CS, CDen62-*g*-CS20. Huang et al. reported that nanoparticles with a short CS chain (10 kDa) were unexpectedly larger than those produced from CS of a molecular mass in the range

Table 1
The physicochemical properties of insulin/CDen-*g*-CS nanocomplexes.

Sample	CS (kDa)	DMF[a] (%)	CDen[b] (μmol/g)	Average diameters (nm)	Zeta potential (mV)	Association efficiency (%)	Loading efficiency (%)	Material/insulin[c] (w/w)
CDen62-g-CS20	20	30	62.3	190.3 ± 2.1	3.7 ± 0.4	72.2 ± 2.4	36.1 ± 1.3	1
CDen62-g-CS20	20	30	62.3	247.7 ± 2.0	15.7 ± 0.2	75.4 ± 4.7	37.7 ± 1.9	2
CDen62-g-CS20	20	30	62.3	328.3 ± 6.6	16.9 ± 0.3	54.8 ± 3.6	13.2 ± 2.5	3
CDen58-g-CS20	20	15	58.5	–	27.1 ± 0.6	68.4 ± 4.6	34.2 ± 4.3	2
CDen52-g-CS20	20	40	52.3	–	31.3 ± 0.5	63.1 ± 1.2	31.6 ± 1.9	2
CDen60-g-CS6	6	30	60.1	266.9 ± 2.2	25.5 ± 1.2	75.0 ± 2.0	18.8 ± 0.8	2
CDen52-g-CS6	6	0	52.3	–	29.7 ± 0.9	69.3 ± 3.1	16.6 ± 1.1	2

[a] The amount of DMF in the reaction solution.
[b] The amount of β-CDen immobilized was determined according to the reference 32.
[c] The pH of the final solution was about 4.3.

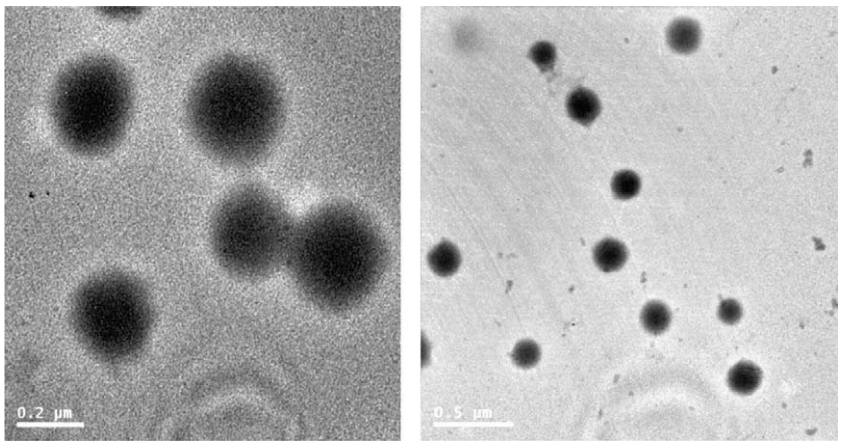

Fig. 5. TEM photographs of insulin/CDen62-*g*-CS20 nanocomplexes (w/w, 1:1).

17–213 kDa, but the mechanism is unclear (Huang, Khor, & Lim, 2004).

The surface charge of nanoparticles was positive in the range of +3.7 to +25.5 mV (Table 1). The data show an increase in zeta potential from +3.7 to +16.9 mV with increasing insulin content from 1 to 3 mg/mL. This was attributed to the part of the positive charged insulin (p*I* 5.3) in acid condition (pH 4.3). Furthermore, the amount of β-CDen grafted had a major influence on the surface charge of nanoparticles; thus, there was a decrease in surface charge from +31.3 to +15.7 mV with an increase in the amount of β-CDen from 52.3 to 62.1 μmol/g (CDen52-*g*-CS20 and CDen62-*g*-CS20), which is due to that β-CD coated as a "brush" on the nanoparticle surface.

Insulin/CDen-*g*-CS nanocomplexes displayed high association efficiency (75.4%), leading to insulin loading capacity as high as 37.7% (Table 1). The association efficiency increased from 63.1% to 75.4% with an increase in the amount of β-CDen immobilized on CS chains from 52.3 to 62.1 μmol/g. These results are probably due to the intensity of the interactions between insulin and the substrate. In fact, these interactions consist of a mixture of host–guest complexation with β-CDen, hydrogen bonding with β-CDen polymer, physical adsorption into the pores (Boschin et al., 2006) and an ionic interaction between CS and insulin.

3.6. In vitro insulin release

Fig. 6A shows the profiles of the cumulative release of insulin from insulin/CDen-*g*-CS nanocomplexes with CS of different molecular mass (CDen62-*g*-CS20 and CDen60-*g*-CS6), and β-CDen content fixed at about 60 μmol/g. The rate of insulin release from two types of nanocomplex particle systems was initially rapid, and then decreased after several hours. This indicates that part of the insulin was adsorbed onto the nanocomplexe surface, and then diffused rapidly when the nanocomplexes came into contact with the release medium. Later, insulin was released slowly due to swelling or degradation of the polymer (Scheme 1).

As can be seen from Fig. 6A, the initial release of insulin from the CDen62-*g*-CS20 nanocomplexes with 20 kDa CS was 31%, and only 49% of the trapped drug was released during 6 h. In contrast, 54% of insulin was released from CDen60-*g*-CS6 nanocomplexes in the same time. To investigate more precisely the effect of the interpolymeric complex formation on release of insulin at pH 7.4, results were analysed according to Ritger–Peppas equation (Eq. (2)) (Ritger and Peppas, 1987) and Higuchi equation (Eq. (3)). In all cases, *n* values were lower than 0.5 (Table 2). These Fickian behaviours may suggest that insulin released from interpolymeric networks is controlled by a drug diffusion process. The faster profile is obtained with the lower molecular mass CS. This can be explained by the fact that the higher molecular mass CS (20 kDa) had longer chain segments, which influenced the diffusion of insulin as well as the rate of degradation of the nanocomplexes.

In addition, it can be seen from Fig. 6B that the rate of insulin release was affected by β-CDen content; increasing β-CDen content from 52.3 to 62.1 μmol/g increased the percentage released from 37.8% to 48.6% within 6 h, which shows the evident roles played by β-CD present on polymer. The first action is to promote the adsorption of the biologically active molecules by CDen-*g*-CS during the impregnation step. This explains why the total doses of insulin released during the batch experiments are so important. Boschin et al. observed that β-CD-grafted Polyvinylidene fluoride membranes increased the release of drug with respect to the raw membranes (Boschin et al., 2006). Moreover, according to Ritger–Peppas equation (Eq. (2)), R^2 was higher than 0.90 and *n* was lower than 0.5 in all cases (Table 2). The fact that we have achieved drug release kinetics is Fickian diffusion. The system CDen52-*g*-CS20 showed slower release profiles than CDen62-*g*-CS20. These profiles are affected by β-CDen content.

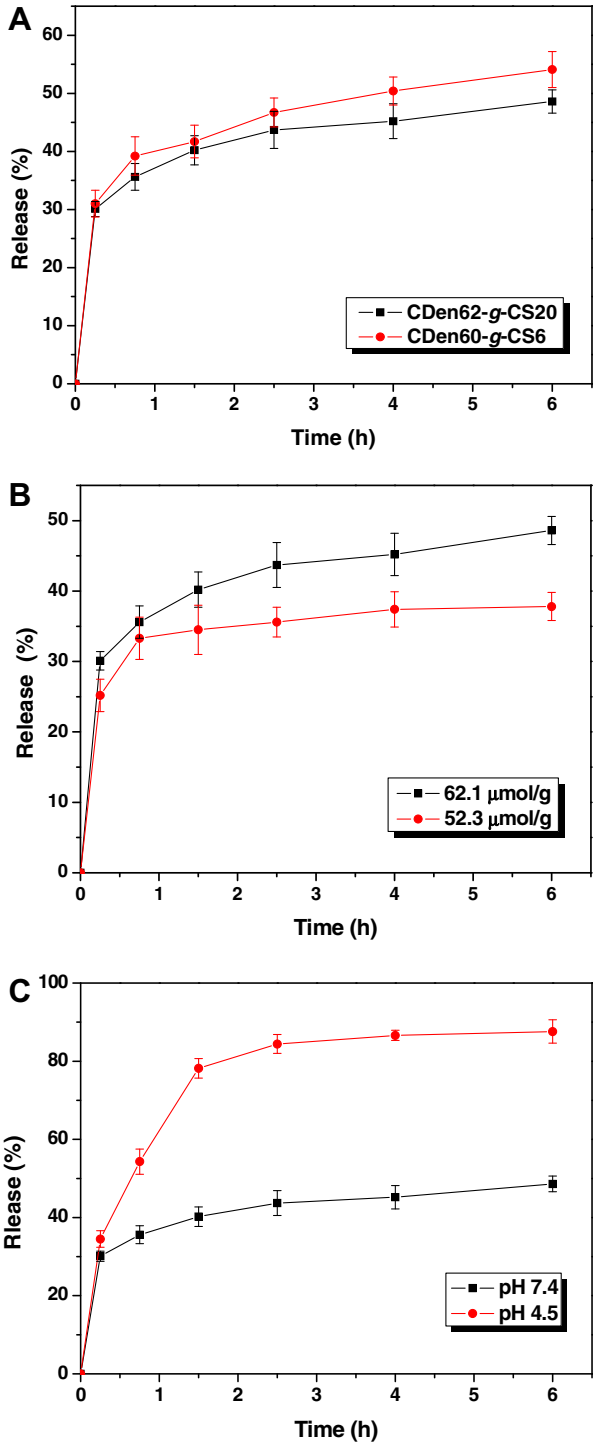

Fig. 6. In vitro percentage cumulative release of insulin from the CDen-*g*-CS nanocomplexes: (A) The effect of chitosan molecular masses on the insulin release in PBS of pH 7.4; (B) The effect of the amount of β-CD immobilized on the insulin release in PBS of pH 7.4; (C) The effect of pH on the insulin release from CDen62-*g*-CS20 nanocomplexes. Triplicates for each sample were analyzed and each datum point represents the mean value ± SD ($n = 3$).

The release profiles of insulin from complexes formed with CDen62-*g*-CS20 were investigated at acetic acid/sodium acetate buffer (pH 4.5) and phosphate buffer solution (pH 7.4), respectively. Fig. 6C shows insulin was released very rapidly at pH 4.5 and 80% insulin was released after 6 h, while at pH 7.4, a much

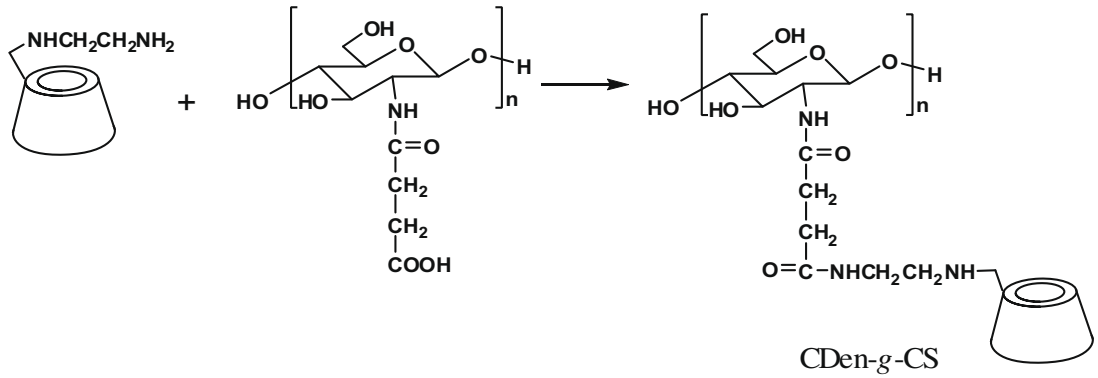

Scheme 1. The synthesis of CDen-grafted chitosan.

Table 2
Drug release kinetic data for CDen-*g*-CS nanocomplexes obtained from fitting drug release experimental data to Higuchi and Ritger–Peppas equation (*n*: diffusion exponent, k_1 and k_2: kinetic constants, R^2: correlation coefficient).

Sample	pH of release media	Higuchi model		Ridger–Peppas model			Transport mechanism
		k_1	R^2	n	k_1	R^2	
CDen62-g-CS20	pH 7.4	1.1820	0.9391	0.1484	37.3760	0.9907	Diffusion controlled
CDen60-g-CS6	pH 7.4	1.4644	0.9591	0.1701	39.8375	0.9900	Diffusion controlled
CDen52-g-CS20	pH 7.4	0.7549	0.8061	0.1164	32.0306	0.9060	Diffusion controlled
CDen62-g-CS20	pH 4.5	3.4464	0.7353	–	–	–	–

slower release was observed. This significant difference of insulin release with the change in medium pH is also resulted from the insulin ionization. The loaded insulin is positively charged at pH 4.5 as mentioned above, thus interacted with the positive CDen-*g*-CS, rending complexes dissociation due to electrostatic repulsion, leading to a rapid release. In contrast, the insulin charge becomes negative at pH 7.4 and less than 50% insulin was released from the complexes at pH 7.4 buffer within 6 h. However, the drug release kinetic at pH 4.5 was not agreement with Ritger–Peppas and Higuchi model. In fact, the diffusion process could play as much an important role in the release of insulin as the dissolution processes do at pH 4.5.

4. Conclusions

Insulin/CDen-*g*-CS nanocomplexes have shown an excellent capacity for the association of insulin and displayed insulin release kinetics and properties. The insulin release was influenced by changing the composition of CDen-*g*-CS and pH of release medium, which made them very interesting systems for drug delivery. Moreover, CDen-*g*-CS kept the stability of insulin compared with control insulin solution. And the cell viability study shows that CDen-*g*-CS possessed the good biocompatibility. In conclusion, CDen-*g*-CS has the potential to apply in the drug delivery for peptides and proteins as an efficient delivery vehicle.

Acknowledgement

The starting projects for young teachers from the Ministry of Education, for financial support are gratefully acknowledged.

References

Aachmann, F. L., Otzen, D. E., Larsen, K. L., & Wimmer, R. (1999). Structural background of cyclodextrin–protein interactions. *Protein Engineering, 16*, 905–912.

Aoki, N., Nishikawa, M., & Hattori, K. (2003). Synthesis of chitosan derivatives bearing cyclodextrin and adsorption of *p*-nonylphenol and bisphenol A. *Carbohydrate Polymers, 52*, 219–223.

Boschin, F., Blanchemain, N., Bria, M., Delcourt-Debruyne, E., Morcellet, M., Hildebrand, H. F., et al. (2006). Improved drug delivery properties of PVDF membranes functionalized with β-cyclodextrin-application to guided tissue regeneration in periodontology. *Journal of Biomedical Materials Research Part A, 79A*, 78–85.

Chen, S. P., & Wang, Y. T. (2001). Interaction of *n*-alkanes with crosslinked cis-1, 4-polybutadiene. *Journal of Applied Polymer Science, 82*, 2414–2421.

Dotsikas, Y., & Loukas, Y. L. (2002). Kinetic degradation study of insulin complexed with methyl-beta cyclodextrin. *Journal of Pharmaceutical and Biomedical Analysis, 29*, 487–494.

Dubois, M., Gilles, K. A., Hamilton, J. K., Rebers, P. A., & Smith, F. (1956). Colorimetric methods for the determination of sugar and related substances. *Analytical Chemistry, 28*, 350–356.

El-Tahlawy, K., Gaffar, M. A., & El-Rafie, S. (2006). Novel method for preparation of β-cyclodextrin/grafted chitosan and it's application. *Carbohydrate Polymers, 63*, 385–392.

Filipović-Grčić, J., Voinovich, D., Moneghini, M., Bećirević-Laćan, M., Magarotto, L., & Jalšenjak, I. (2000). Cyclodextrin inclusion complex. *European Journal of Pharmaceutical Sciences, 9*, 373–379.

Gaffar, M. A., El-Rafie, S. M., & El-Tahlawy, K. F. (2004). Preparation and utilization of ionic exchange resin via graft copolymerization of β-CD itaconate with chitosan. *Carbohydrate Polymers, 56*, 387–396.

Hirano, S., & Moriyasu, T. (1981). *N*-(Carboxyacyl)chitosans. *Carbohydrate Research, 92*, 323–327.

Holme, K., & Hall, L. D. (1992). Preparation and characterization of *N*-[2-(glycosyloxy)-ethyl]chitosan derivatives. *Carbohydrate Research, 225*, 291–306.

Huang, M., Khor, E., & Lim, L. Y. (2004). Uptake and cytotoxicity of chitosan molecules and nanoparticles: Effects of molecular weight and degree of deacetylation. *Pharmaceutical Research, 21*, 344–353.

Illum, L., Farraj, N. F., & Davis, S. S. (1994). Chitosan as a novel nasal delivery' system for peptide drugs. *Pharmaceutical Research, 11*, 1186–1189.

Irie, T., & Uekama, K. (1997). Pharmaceutical applications of cyclodextrins III toxicological issues and safety evaluation. *Journal of Pharmacological Sciences, 86*, 147–162.

Irie, T., & Uekama, K. (1999). Cyclodextrins in peptide and protein delivery. *Advanced Drug Delivery Reviews, 36*, 101–123.

Kurita, K. (2001). Controlled functionalization of the polysaccharide chitin. *Progress in Polymer Science, 26*, 1921–1971.

Liu, Y., Yang, Y. W., Cao, R., Song, S. H., Zhang, H. Y., & Wang, L. H. (2003). Thermodynamic origin of molecular selective binding of bile salts by aminated β-cyclodextrins. *Journal of Physical Chemistry B, 107*, 14130–14139.

Lovatt, M., Cooper, A., & Camilleri, P. (1996). Energetics of cyclodextrin. Induced dissociation of insulin. *European Biophysics Journal, 24*, 354–357.

Matsubara, M., Ando, Y., Iri, T., & Uekama, K. (1997). Protection afforded by maltosyl-β-cyclodextrin against α-chymotrypsin-catalyzed hydrolysis of a luteinizing hormone-releasing hormone agonist, buserelin acetate. *Pharmaceutical Research, 14*, 1401–1405.

Merkus, F. W. H. M., Verhoef, J., Romeijn, S. G., & Schipper, N. G. M. (1991). Absorption enhancing effect of cyclodextrins on intranasally administered insulin in rats. *Pharmaceutical Research, 8*, 588–592.

Moses, L. R., Dileep, K. J., & Sharma, C. P. (2000). Beta cycodextrin-insulin encapsulated chitosan/alginate matrix: oral delivery system. *Journal of Applied Polymer Science, 75*, 1089–1096.

Ogawa, K., Hirano, S., Miyanishi, T., Yui, T., & Watanabe, T. (1984). A new polymorph of chitosan. *Macromolecules, 17*, 973–975.
Peppas, N. A. (1985). Analysis of Fickian and non-Fickian drug release from polymers. *Pharmaceutica Acta Helvetiae, 60*, 110–111.
Petter, R. C., Salek, J. S., Sikorski, C. T., Kumaravel, G., & Lin, F. (1990). Cooperative binding by aggregated mono-6-(alkylamino)-β-cyclodextrins. *Journal of the American Oil Chemists' Society, 112*, 3860–3868.
Pocker, Y., & Biswas, S. B. (1980). Conformational dynamics of insulin in solution: circular dichroic studies. *Biochemistry, 19*, 5043–5049.
Prabaharan, M., & Mano, J. F. (2005). Hydroxypropyl chitosan bearing β-cyclodextrin cavities: Synthesis and slow release of its inclusion complex with a model hydrophobic drug. *Macromolecular Bioscience, 5*, 965–973.
Prabaharan, M., & Mano, J. F. (2006). Chitosan derivatives bearing cyclodextrin cavities as novel adsorbent matrices. *Carbohydrate Polymers, 63*, 153–166.
Qu, X., Wirsen, A., & Albertsson, A. C. (2000). Novel pH sensitive chitosan hydrogel swelling behavior and states of water. *Polymer, 41*, 4589–4598.
Ravi, K., & Majeti, N. V. (2000). A review of chitin and chitosan applications. *Reactive and Functional Polymers, 46*, 1–27.
Saito, H., Ryoko, T., & Ogawa, K. (1987). High-resolution solid-state ^{13}C NMR study of chitosan and its salts with acids. *Macromolecules, 20*, 2424–2430.
Sajeesh, S., & Sharma, C. P. (2006). In vitro binding of ketamine to human serum albumin. *International Journal of Pharmaceutics, 25*, 147–153.
Sakr, F. M. (1996). Nasal administration of glycagon combined with dimethyl-β-cyclodextrin: comparison of pharmacokinetics and pharmacodynamics of spray and powder formulations. *International Journal of Pharmaceutics, 132*, 189–194.
Samuels, R. J. (1981). Solid state characterization of the structure of chitosan films. *Journal of Polymer Science. Polymer Physics Ed, 19*, 1081–1105.
Tozaki, H., Komoike, J., Tada, C., Maruyama, T., Terabe, A., Suzuki, T., et al. (1997). Chitosan capsules for colon specific drug delivery: improvement of insulin absorption from the rat colon. *Journal of Pharmacological Sciences, 86*, 1016–1021.
van der Lubben, I. M., Verhoef, J. C., Borchard, G., & Junginger, H. E. (2001). Chitosan and its derivatives in mucosal drug and vaccine delivery. *European Journal of Pharmaceutical Sciences, 14*, 201–207.
Venter, J. P., Kotźe, A. F., Auźely-Velty, R., & Rinaudo, M. (2006). Synthesis and evaluation of the mucoadhesivity of a CD-chitosan derivative. *International Journal of Pharmaceutics, 313*, 36–42.
Victor, P. V., & Sharma, C. P. (2002). Stimuli sensitive polymethacrylic acid microparticles (PMAA)-oral insulin delivery. *Journal of Biomaterials Applications, 17*, 125–134.
Vilivalam, V. D., & Dodane, V. (1998). Pharmaceutical applications of chitosan. *Pharmaceutical Science and Technology Today, 1*, 246–253.
Yang, T., Hussain, A., Paulson, J., Abbruscato, T. J., & Ahsan, F. (2004). Cyclodextrins in nasal delivery of low-molecular-weight heparins: in vivo and in vitro studies. *Pharmaceutical Research, 21*, 1127–1136.
Yang, C., Li, H., Goh, S. H., & Li, J. (2007). Cationic star polymers consisting of alpha-cyclodextrin core and oligoethylenimine arms as non-viral gene delivery vectors. *Biomaterials, 28*, 3245–3254.